PHASE ROTATION AT THE FRONT END OF A NEUTRINO FACTORY

Harold Kirk*, Juan Gallardo, Robert Palmer, BNL, Upton, NY 11973, USA
Michael Green, Lou Reginato, Simon Yu, LBNL, Berkeley, CA 94720, USA
Dan Kaplan, IIT, Chicago, IL 60616 USA
Yasuo Fukui, UCLA, Los Angeles, CA 90095 USA

Abstract

The muon collection scheme for a muon-storage-ring-based Neutrino Factory consists of a target irradiated with a 1 MW proton beam followed by a 30-m decay channel and then a 300-m long induction linac phase rotation. The purpose of the induction-linac section is to reduce the $\delta E/E$ spread of the collected muons to a value which is manageable for the subsequent buncher and cooling sections. We describe in this paper the overall design concept of the phase-rotation system and give key parameters for the induction linacs.

1 INTRODUCTION

The function of the phase-rotation section of the Neutrino Factory is to reduce the energy spread of the collected muon beam to a manageable level which will allow reasonable throughput to subsequent system components. In Fig. 1, we show the proposed layout of the phase-rotation section followed by the buncher and cooling sections. Figure 2 shows the longitudinal structure of the beam after the application of our proposed three-stage phase-rotation system.

For a Neutrino Factory, the longitudinal phase space requirements are quite different than that for a Muon Collider. Unlike the Muon Collider case, we can permit the captured muon beam to grow in its longitudinal dimensions. We then put the beam through a buncher system which will allow the subsequent cooling section to be operated with higher-frequency rf cavities than would otherwise be possible.

If the process is done with a single drift and single induction linac [1], then relativistic effects cause a distortion of the rotated bunch such that the initially high-energy particles emerge with a larger energy spread than those with initially low energy. The use of at least two induction linacs [2], with a drift between them, allows this distortion to be greatly reduced.

It is natural for each induction linac to be bipolar, however, such bipolar voltage pulses have been avoided in our design. In the case of the first linac, a subsequent hydrogen absorber reduces the beam energy, allowing this first linac to be unipolar. This absorber also reduces the normalized emittance, and is thus referred to as a "mini-cooler." To avoid a bipolar second linac, we substitute it with two linacs: the first unipolar-decelerating, the second unipolar-accelerating.
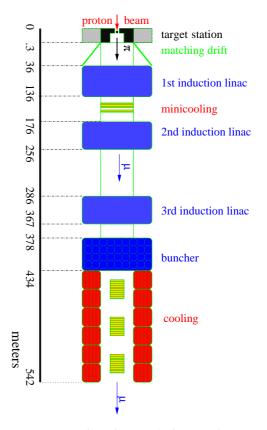

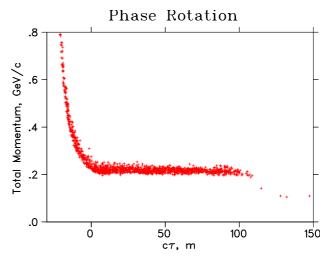Figure 1: Layout of the front end of a Neutrino Factory

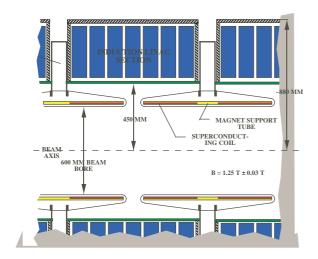Figure 2: Beam longitudinal profile after phase rotation

---

* hkirk@bnl.gov

Figure 3: Longitudinal section showing placement of solenoid coils within an induction cell.

Figure 4: Acceleration waveforms for induction linacs 1, 2 and 3

2 DRIFT SECTIONS

A principle strategy for the drift sections of the capture/decay channel is to avoid the π resonances which will be present due to the periodic structure of the solenoidal magnetic field resulting from the necessary gaps between the superconducting coils. These π-resonance points are approximated by

$$p = \lambda \frac{Bc}{2\pi n}$$

where p is in units of eV/c, B is the average solenoidal field in Tesla, c is the speed of light in m/sec and the period λ is in meters.

We note that if we wish to avoid losses of particles in the momentum region of 100 to 300 MeV/c then a channel based on a 1.25-T solenoidal field and a 50-cm period is suitable. We extend this periodicity throughout the capture channel to include also the induction linacs (see Fig. 3). Only the minicool section with its single-flip solenoidal field does not exhibit this 50-cm periodicity. Using ICOOL [3] we have compared the results of transporting MARS-generated [4] particles from the target through the exit of the third induction linac for both the case of 50-cm periodicity and an artificial flat 1.25-T solenoidal field throughout the channel (excluding the minicool segment). We find that the total throughput of muons at the exit of the third induction linac is the same for both cases.

3 INDUCTION LINAC SECTIONS

The three linear induction-accelerator sections consist of simple nonresonant structures where the drive voltage is applied to an axially-symmetric gap that encloses a toroidal ferromagnetic material. The change in flux in the magnetic core induces an axial electric field that accelerates the muon beam. Th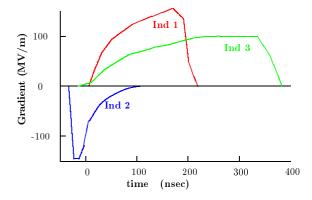is simple non-resonant (low-Q) structure acts as a single-turn transformer. Each section is typically a low-gradient structure that can provide acceleration fields of varying shapes and time durations from tens of nanoseconds to several microseconds. The acceleration voltage available is simply given by the expression $V = AdB/dt$. Hence, for a given cross-sectional area of material (A), the duration of the beam pulse influences the energy gain. Furthermore, a premium is put on minimizing the diameter, which impacts the total weight or cost of the magnetic material. The diameter doubly impacts the cost since the power to drive the cores is proportional to the volume as well.

We have optimized the waveforms and linac lengths in order to provide the most favorable $\delta E/E$ ratio at the end of the phase-rotation channel. The resulting acceleration waveforms are shown in Fig. 4 and key induction-linac parameters are given in Table 1. From a projection of Fig. 2 we obtain $\delta E/E = 4.4\%$.

Table 1: Induction accelerator parameters

		1	2	3
length	m	100	80	80
inner radius	cm	30	30	30
solenoid field	T	1.25	1.25	1.25
maximum gradient	MV/m	1.55	1.45	1.0
pulse length	ns	190	100	360

Although the second and third induction linacs can be combined into one by utilizing a bipolar pulse, we feel that it is preferable to reduce the risk factors by separating the two functions with a small penalty in economics. Combining the second and third sections would require the application of "branched magnetics" to achieve two waveforms that are independently controllable in shape and timing. The branched-magnetics approach could lead to a cost savings but at more risk since this approach has only been applied to small bench-top prototypes but not to currently-

operating induction accelerators.

The induction accelerators are driven by pulse generators with output voltages from 100-200 kV, currents in the tens of kiloamperes, and pulse durations from 50 ns to 300 ns. The peak-power levels exceed one gigawatt and, except for spark gaps, no switches exist which can operate reliably at the required repetition rates and power levels. Since spark gaps are not acceptable, we consider here a nonlinear magnetic pulse-compression modulator.

The use of saturable reactors for generating very high peak power levels was described by Melville [5]. The basic principle behind magnetic pulse switching is to use the large changes in permeability exhibited by saturating ferri- or ferro-magnetic materials to produce large changes in impedance. By using multiple stages, it is possible to compress a pulse of relatively low power and long duration into a pulse of very high peak power and very short duration while maintaining the same energy (except for a small core loss) per pulse. With this technique we can use available thyratrons or solid-state devices to initiate the pulse and then pulse-compress it to the desired peak power level.

4   THE ABSORBERS

The absorber is divided in two parts with a field reversal between them to avoid the generation of angular momentum. The baseline design includes two liquid-hydrogen absorbers, each 30 cm in radius and 1.75 m long. Simulations have been used to propagate MARS-generated secondary particles from the primary target through the initial induction-linac module to the absorbers. Table 2 gives the estimated power deposition for each important particle species generated at the target (≈ 5 kW for each absorber). As seen in Fig. 5, the power dissipation in the first absorber is peaked at the absorber's upstream end. This energy-dissipation peak is due to the arrival of low-energy protons which are generated at the target and conducted down the capture/decay channel. They are not removed by the induction linac because they are out of time with the higher-velocity mesons and electrons. A beryllium sheet placed immediately before the liquid-hydrogen absorber would act to absorb the low-energy protons and reduce the peak energy deposition in the first several cm of liquid hydrogen. Nevertheless, even without this beryllium buffer, we find the volume power density in the liquid hydrogen to be acceptable.

Table 2: Power dissipation in the first minicool absorber.

	Power, KW				
	e	μ	π	K	p
positives	0.42	2.02	0.14	0	0.86
negatives	0.43	1.29	0.24	0	-

We can be confident about the overall power-handling capability of these absorbers based on experience with
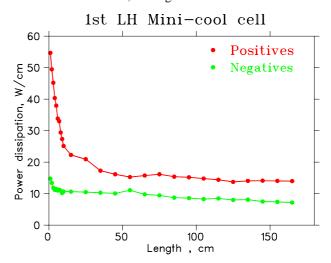

Figure 5: Power deposition along the length of the first minicool absorber.

the Fermilab 15-foot bubble chamber which was cooled by a 6.7 kW refrigerator. While considerably larger than a minicooling absorber, it had substantially lower beam-induced power dissipation; the large refrigeration plant was required due to the work done on the fluid by the rapid-cycling expansion piston.

The liquid-hydrogen target built for SLAC Experiment 158 [6],[7] is designed to handle 700 W, uniformly distributed over 1.5 m of length but with ≈ 1 mm r.m.s. transverse beam size. While the power/cm at the upstream end of the first minicooling absorber is more than 10 times that in SLAC E158, the power/cm^3 is only about 10^{-3} of that in E158. We therefore conclude that the peak power density will not pose a problem.

5   REFERENCES

[1] *A Neutrino Source Based on an Intense Muon Storage Ring*, ed. N. Holtkamp and D. Finley, Fermilab-Pub-00/108-E(2000). http://www.fnal.gov/projects/muon_collider/nu-factory/nu-factory.html

[2] *Feasibility Study-II of a muon-based neutrino source*, ed. S. Ozaki R. Palmer,M. Zisman, and J. Gallardo, 2001, BNL-52623. http://www.cap.bnl.gov/mumu/studyii/final_draft/

[3] R.C. Fernow, *A simulation code for ionization cooling of muon beams*, Proceedings of the 1999 Particle Accelerator Conference, March 1999, p.3020.

[4] N.V. Mokhov et al., Fermilab-Conf-98/379LANL Report LA-UR-98-5716(1998); http://www-ap.fnal.gov/MARS/

[5] W.S. Melville *The Use of Saturable Reactors as Discharge Devices for Pulse Generators* The Institution of Electrical Engineers. Vol. 98, Part III, No. 53. May 1951.

[6] R. W. Carr et al., SLAC-Proposal-E-158, July 1997.

[7] R. W. Carr et al., *E158 Liquid Hydrogen Target Milestone Report*, April 21, 1999.
http://www.slac.stanford.edu/exp/e158/documents/target.ps.gz.